Realization of nonequilibrium thermodynamic processes using external colored noise

Pau Mestres,[1] Ignacio A. Martinez,[1] Antonio Ortiz-Ambriz,[1,2] Raul A. Rica,[1,*] and Edgar Roldan[1,3,†]

[1]*Institut de Ciències Fotòniques (ICFO), Mediterranean Technology Park, Av. Carl Friedrich Gauss, 3, 08860 Castelldefels (Barcelona), Spain*

[2]*Photonics and Mathematical Optics Group, Tecnológico de Monterrey, 64849 Mexico*

[3]*Grupo Interdisciplinar de Sistemas Complejos (GISC), Madrid, Spain*

(Received 12 June 2014; published 16 September 2014)

We investigate the dynamics of single microparticles immersed in water that are driven out of equilibrium in the presence of an additional external colored noise. As a case study, we trap a single polystyrene particle in water with optical tweezers and apply an external electric field with flat spectrum but a finite bandwidth of the order of kHz. The intensity of the external noise controls the amplitude of the fluctuations of the position of the particle and therefore of its effective temperature. Here we show, in two different nonequilibrium experiments, that the fluctuations of the work done on the particle obey the Crooks fluctuation theorem at the equilibrium effective temperature, given that the sampling frequency and the noise cutoff frequency are properly chosen.

DOI: 10.1103/PhysRevE.90.032116 PACS number(s): 05.70.Ln, 05.20.−y, 05.40.−a, 42.50.Wk

I. INTRODUCTION

The thermodynamics of small systems is strongly affected by the thermal fluctuations of the surroundings [1]. Although often looked at as an unwanted source of noise, fluctuations also bring to life phenomena such as stochastic resonances [2], temporal violations of the Second Law of Thermodynamics [3], or the possibility to build engines at the microscale of a greater efficiency than that of their macroscopic counterparts [4–6].

At the microscale, the amplitude of the fluctuations of the thermodynamic quantities depends on the temperature of the environment. Unfortunately, temperature control has remained challenging due to the difficulties found in isolating microscopic systems and the presence of convection effects in fluids [7,8]. In Ref. [7] a thermal collar was attached to an objective in order to heat up a sample fluid. In a different approach, a laser line matching the absorption peak of water was used to heat the sample uniformly, thus avoiding convection [5]. Although the aforementioned methods were proved capable of controlling the temperature, they were limited to increase the temperature of the sample in a range of tens of Kelvins.

To overcome the short range of accessible temperatures, it has been suggested that random forces can mimic a thermal bath for colloidal particles [9–11]. In fact, the existence of fluctuations in the small scale is due to neglected degrees of freedom in the description of the system [9]. In other words, thermal fluctuations are produced by the constant exchange of energy between the system under consideration and the $\sim N_A$ molecules of the surrounding environment, N_A being the Avogadro number. In Ref. [10] it was shown that the Crooks work fluctuation theorem [12] fails if one assumes that external random forces exert work on a colloidal particle. Therefore, by virtue of the First Law of Thermodynamics, the energy transferred by external random forces should be interpreted as *heat*.

Martínez *et al.* first tested such interpretation experimentally [11] by observing that a colloidal particle subject to an external random force with Gaussian white spectrum behaves as if it were immersed in a thermal bath whose effective temperature exceeds that of the surrounding fluid. The concept of effective temperature was previously introduced as a parameter that measures the deviation from the fluctuation-dissipation relation at room temperature [13] in glassy and amorphous materials [14–16], granular media [17], or active matter [18,19]. However, deviations between the effective temperatures in equilibrium and in nonequilibrium processes were found that make dubious whether using random forces is suitable to mimic a thermal bath.

Optical tweezers offer a robust and versatile platform for micromanipulation [8,20–24] and for the study of the thermodynamics of systems where fluctuations cannot be neglected [1,9,25]. Interestingly, it can be easily combined with other experimental techniques in order to broaden its applicability. For example, optical trapping has been combined with Raman spectroscopy [26,27] or fluorescence microscopy [28] to study single molecule biology. When the trapped objects are charged, the application of electric fields can be used to perform single particle electrophoresis [29–32] or study the fundamental laws of thermodynamics at small scales [4,33,34].

In this article, we extend the use of random forces to mimic a thermal bath for a colloidal particle undergoing nonequilibrium processes in an optical trap. In particular, we analyze the validity of the interpretation of a noisy electric force as a heat bath in out-of-equilibrium dragging and expansion-compression processes. With data from both experiments and numerical simulations, we demonstrate that the observed mismatch between equilibrium and nonequilibrium kinetic temperatures can be caused by an inappropriate sampling rate during the experiment. We show that the fluctuations of thermodynamic quantities are very sensitive to the sampling frequency and to the actual properties of the external noise, which in practice will always be colored.

The article is organized as follows. In Sec. II we discuss the theoretical extension of the Crooks fluctuation theorem to

*rul@ugr.es
†edgar.roldan@fis.ucm.es

small systems driven by external random forces. In Sec. III we describe the experimental setup and the protocols that we use to implement nonequilibrium processes with external colored noise. In Sec. IV we show and discuss the experimental results obtained in the implementation of two different nonequilibrium processes with a trapped colloidal particle, proposing an optimal sampling rate to realize nonequilibrium processes with our setup. Section V gives the concluding remarks of our work.

II. CROOKS FLUCTUATION THEOREM UNDER RANDOM DRIVING

Let us consider a Brownian colloidal particle that moves in one dimension x and is immersed in a thermal bath at temperature T. The particle is trapped with a quadratic potential centered at the position $x = x_0$, $U(x,x_0,\kappa) = \frac{1}{2}\kappa(x - x_0)^2$, κ being the stiffness of the trap. The position of the particle obeys the overdamped Langevin equation [35],

$$\gamma\dot{x}(t) = -\kappa(t)[x(t) - x_0(t)] + \xi(t) + \eta(t), \tag{1}$$

where γ is the friction coefficient and both the stiffness and the position of the trap can change with time t. The term $\xi(t)$ is a stochastic force that accounts for the random impacts of the molecules in the environment with the particle, responsible for its Brownian motion, which is modeled by a Gaussian white noise of zero mean $\langle\xi(t)\rangle = 0$ and correlation $\langle\xi(t)\xi(t')\rangle = 2\gamma kT\delta(t - t')$. We also consider the possibility that an additional external random force $\eta(t)$ is applied to the particle, which satisfies $\langle\eta(t)\rangle = 0$ and $\langle\eta(t)\eta(t')\rangle = \sigma^2\Gamma(t - t')$, where $\Gamma(t - t')$ is the correlation function of the force and σ its amplitude. In the general case, this correlation function is different from a δ function.

In the absence of external forces and being κ and x_0 fixed at a constant value, the fluctuations of the position of the particle are Gaussian distributed. The amplitude of these fluctuations depends on the temperature of the surroundings, as predicted by the equipartition theorem, $\kappa\langle(x - x_0)^2\rangle = kT$, where the brackets denote steady-state averaging. If we also include the external random force $\eta(t)$, the equipartition theorem allows us to define a kinetic temperature of the particle from the amplitude of its motion:

$$T_{\text{kin}} = \frac{\kappa\langle(x - x_0)^2\rangle}{k}. \tag{2}$$

If $\eta(t)$ has the same nature as the Brownian force, i.e., it is described by a Gaussian white noise, then $T_{\text{kin}} = T + \frac{\sigma^2}{2k\gamma}$. Otherwise, the relation between T_{kin} and the noise intensity is more complex and depends on the characteristic time scales of the particle [11]. However, it always verifies $T_{\text{kin}} \geqslant T$ [11,33].

Let us now consider a thermodynamic process along which an external agent can change the energy of the Brownian particle via a control parameter λ that can be arbitrarily switched in time, for instance, the stiffness of the trap. The duration of the process is τ and the control parameter follows a protocol $\{\lambda_t\}_{t=0}^{\tau} \equiv \{\lambda(t)\}_{t=0}^{\tau}$. For convenience, we also consider the *time-reversal* process, described by $\{\tilde{\lambda}_t\}_{t=0}^{\tau} = \{\lambda_{\tau-t}\}_{t=0}^{\tau}$. We assume that the system is initially in canonical equilibrium state and is allowed to relax to equilibrium at the end of the process. The position of the particle is random and describes a stochastic *trajectory*, $\{x_t\}_{t=0}^{\tau} \equiv \{x(t)\}_{t=0}^{\tau}$. Along the process, the external agent exerts work on the particle, which depends on the trajectory of the particle [9],

$$W = \int_0^{\tau} \frac{\partial U(x_t,\lambda_t)}{\partial\lambda_t} \circ d\lambda_t, \tag{3}$$

where $\circ$ denotes Stratonovich product. Stratonovich product consists in using the following prescription of the integral of a function of a stochastic variable x:

$$\int_0^{\tau} f(x_t) \circ dy_t = \sum_t \frac{f(x_t) + f(x_{t+\Delta t})}{2}(y_{t+\Delta t} - y_t), \tag{4}$$

y being a second (stochastic or deterministic) variable, Δt the time between two samplings, and t runs from $t = 0$ to $t = \tau - \Delta t$ [9].

The average of the work over many different realizations yields the classical result $\langle W\rangle \geqslant \Delta F$, where ΔF is the free energy difference between the final and initial (equilibrium) states of the system [9]. The fluctuations of the work are not symmetric upon time reversal of the protocol if the system is driven out of equilibrium, as first shown by Crooks [12]. For an arbitrarily far-from-equilibrium process, the work distribution of the *forward* process $\rho(W)$ is related to the distribution of the work in the *backward* (time-reversal) process, $\tilde{\rho}(W)$,

$$\frac{\rho(W)}{\tilde{\rho}(-W)} = \exp\left(\frac{W - \Delta F}{kT}\right). \tag{5}$$

Equation (5) is known as the Crooks fluctuation theorem (CFT) and is valid when initial and final states are both equilibrium canonical states. CFT was first tested experimentally in DNA pulling experiments [36]. One can also define the following *asymmetry function* [37],

$$\Sigma(W) \equiv \ln\frac{\rho(W)}{\tilde{\rho}(-W)}, \tag{6}$$

which measures the distinguishability between the forward and backward work histograms. CFT can be rewritten in terms of the asymmetry function,

$$\Sigma(W) = \frac{W - \Delta F}{kT}. \tag{7}$$

In the presence of an external random force, CFT is not satisfied if the external force is considered to exert work on the particle [10]. However, if the energy input by the random force is considered as heat, that is, random forces are not included in the calculation of the work, the following modified CFT is satisfied [9]:

$$\Sigma(W) = \frac{W - \Delta F}{kT_c}, \tag{8}$$

where T_c is an effective nonequilibrium temperature called the *Crooks temperature* that is, in general, different to the temperature of the surroundings, T. Equation (8) implies that T_c can be calculated from the slope of $\Sigma(W)$ as a function of W. The value of the effective Crooks temperature depends strongly on the properties of the external noise. In general, T_c and its equilibrium counterpart T_{kin} do not coincide. However, if the external force is an external Gaussian white noise, $T_c = T_{\text{kin}}$ [11].

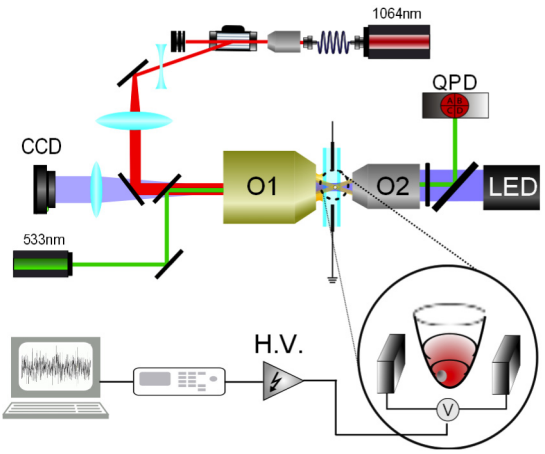

FIG. 1. (Color online) Experimental setup described in Sec. III A. A polystyrene sphere of radius $R = 500$ nm is immersed in a microfluidic chamber filled with water and trapped with an infrared laser using a high numerical aperture objective. Random forces are exerted using a Gaussian white noise process applied to two electrodes placed at the two ends of the chamber. The position is detected projecting the forward scattered light of a green laser in a quadrant photodiode.

III. EXPERIMENTAL METHODS

A. Experimental setup

Our experimental setup, shown in Fig. 1, was previously described in Ref. [11]. We use a 40× objective to collimate the laser beam from a single-mode fiber laser (ManLight ML10-CW-P-OEM/TKS-OTS, 3W maximum power) and send it through an Acousto Optic Deflector (AOD). After the AOD, the beam is expanded with two lenses that also conjugate the center of the AOD crystal with the entrance of a 100× objective (Nikon, CFO PL FL NA1.3) (O1) that creates the field gradient for the optical trap.

For position detection a $\lambda = 532$ nm fiber laser is expanded with a 10× objective and sent through the same objective of the optical trap (O1). The forward scattered light is collected with a 20× (O2) objective and sent to a quadrant photodiode with 50 kHz acquisition bandwidth and nanometer accuracy.

Our sample consists of polystyrene microspheres of diameter $D = (1.00 \pm 0.05)\,\mu$m (PPs-1.0, G. Kisker Products for Biotechnology) injected into a custom-made electrophoretic chamber that can be moved using a piezoelectric stage (Piezosystem Jena, Tritor 102) [38].

The intensity and position of the trap center can be controlled by changing the modulation voltage (V_κ) and the driving voltage of the AOD ($V_{\rm AOD}$), respectively. In order to know the position of the trap and its stiffness we need to obtain the calibration factors between V_κ and κ as well as between $V_{\rm AOD}$ and x_0. First, we measure κ by fitting the power spectral density of the position of a trapped bead to a Lorentzian function [39] at different values of V_κ. Second, the calibration of x_0 as a function of $V_{\rm AOD}$ is obtained from the analysis of the average position of a trapped bead in equilibrium, for different values of $V_{\rm AOD}$ (data not shown).

The external random electric field is generated from a Gaussian white noise process. The sequence was obtained using independent random variables as described in Ref. [11]. The signal from the generator is amplified and applied directly to the two electrodes connected at the two ends of the electrophoretic chamber. Notice that the noise spectrum is flat up to a cutoff frequency of 10 kHz (given by the amplifier), which exceeds by one order of magnitude the cutoff frequency used in Ref. [11].

B. Protocols

We consider two different nonequilibrium processes. First, we study the dynamics of a microscopic sphere in an optical trap that is dragged at constant velocity. Next, we realize a process where the trap center is held fixed but the stiffness of the trap is changed with time.

1. Dragged trap

Our first case study consists of a particle that is driven out of equilibrium by dragging the optical trap of stiffness $\kappa = (18.0 \pm 0.2)$ pN/μm at constant speed $v = 22$ nm/ms. The protocol is shown in Fig. 2 together with a time series of the position of the particle sampled at different acquisition frequencies. First, the trap is held fixed with its center at $x_0 = -55$ nm during $\tau_1 = 7.5$ ms. Then the trap center is displaced in the x axis at a constant velocity from $x_0 = -55$ to 55 nm in a time interval of $\tau_2 = 5$ ms. The bead is then allowed to relax to equilibrium by keeping the trap center fixed at $x_0 = 55$ nm for $\tau_1 = 7.5$ ms before the trap is moved back from $x_0 = 55$ to -55 nm in $\tau_2 = 5$ ms. The duration of each cycle is $\tau = 25$ ms, and every cycle is repeated 12 000 times; that is, the total experimental time was 300 s. Every 300 s cycle is repeated for different values of the amplitude of the random force, starting with the case where no external force is applied.

The relaxation time of the position of the particle is $\tau_r = \gamma/\kappa = 0.5$ ms where $\gamma = 8.4$ pN ms/μm is the friction coefficient calculated using Stokes's law, $\gamma = 6\pi\eta R$, $\eta = 0.89$ mPa s being the viscosity of water at room temperature and $R = 500$ nm the radius of the particle. The time spent

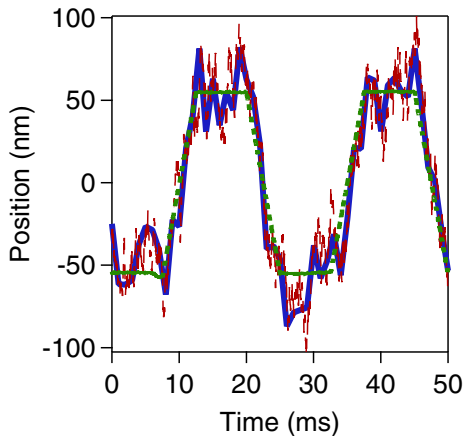

FIG. 2. (Color online) Position of the trap (thick green dashed curve) as a function of time and time traces of the position of the particle sampled at 1 kHz (blue curve) and 10 kHz (thin red dashed curve) in the dragging experiment. The trap moves at a constant velocity of ± 22 nm/ms.

by the trap in the fixed stage of the protocol, τ_1, exceeds by one order of magnitude the relaxation time τ_r, which ensures that the particle reaches equilibrium between the nonequilibrium steps of the protocol. In the dragging steps, the viscous dissipation is of the order of $\langle W_{\rm diss}\rangle \sim \gamma v L$, where $L = 110$ nm is the distance traveled by the trap, which yields $\langle W_{\rm diss}\rangle \sim 20\,{\rm pN\,nm} \simeq 5\,kT$ ($kT \simeq 4$ pN nm at room temperature) indicating that the work dissipation cannot be neglected and the system is therefore out of equilibrium.

In every cycle of the protocol, we calculate the work done on the particle in the forward and backward process using Eq. (3). In this case, the control parameter is the position of the trap center, $\lambda = x_0$, and therefore the work is calculated as

$$W = \int \frac{\partial U}{\partial x_0} \circ dx_0(t) = \int -\kappa[x(t) - x_0(t)] \circ dx_0(t), \quad (9)$$

for every realization of the forward and backward processes.

2. *Isothermal compression and expansion*

As a second application of our technique, we analyze a different thermodynamic process consisting in a "breathing" harmonic potential, where the trap center is held fixed but its stiffness is changed with time from an initial $\kappa_{\rm ini}$ to a final $\kappa_{\rm fin}$ value. Since the stiffness of the trap can be thought of as the inverse characteristic volume of the system, $\kappa \sim 1/V$ [5], such a process is equivalent to an isothermal compression or expansion. At odds with the dragging process, in this case the free energy changes along the process, yielding $\Delta F = kT_{\rm kin} \ln \sqrt{\kappa_{\rm fin}/\kappa_{\rm ini}}$ [9,33].

In the experimental protocol shown in Fig. 3, the trap is initially held fixed with stiffness $\kappa_1 = (16.5 \pm 0.2)$pN/$\mu$m for $\tau_1 = 3.5$ ms. Then, the system is isothermally compressed by increasing the stiffness linearly in time up to $\kappa_2 = (66.8 \pm 0.2)$ pN/μm in $\tau_2 = 2.5$ ms. Further, the particle is allowed to relax to equilibrium for $\tau_1 = 3.5$ ms with the trap stiffness held fixed at κ_2 before the system is isothermally expanded linearly in time from κ_2 to κ_1 in $\tau_2 = 2.5$ ms. Every cycle lasts $\tau = 2(\tau_1 + \tau_2) = 12$ ms and is repeated 24 000 times for different values of the amplitude of the external random force.

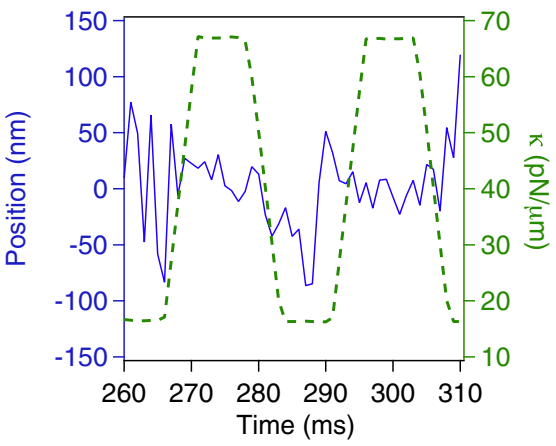

FIG. 3. (Color online) Position of the particle (blue line, left axis) and trap stiffness (green line, right axis) as functions of time in the isothermal compression-expansion cycle. Sampling rate, $f = 1$ kHz.

For every isothermal compression (forward process) and expansion (backward process), we measure the work done on the particle as

$$W = \int \frac{\partial U}{\partial \kappa} \circ d\kappa(t) = \int \frac{1}{2} x^2(t) \circ d\kappa(t), \quad (10)$$

where the control parameter is the trap stiffness in this case [$\lambda = \kappa$ in Eq. (3)].

IV. RESULTS AND DISCUSSION

We now discuss the results obtained when implemented the two different nonequilibrium processes described in Sec. III B. For both processes, we perform a quantitative study of the nonequilibrium work fluctuations of the processes and their time reversals using CFT, as discussed in Sec. II.

A. Dragged trap

Figure 4 shows the work distributions at different noise intensities for both forward and backward dragging processes. When increasing the noise amplitude, the average work remains constant but the variance increases. Since in this process, the free energy does not change, $\Delta F = 0$, then the average work coincides with the average dissipation rate $\langle W\rangle = \langle W_{\rm diss}\rangle$. Therefore, the addition of the external random force does not introduce an additional source of dissipation and can be treated as a heat source. The work distributions at different noise amplitudes fit to theoretical Gaussian distributions obtained from Refs. [11,40] using as the only fitting parameter the nonequilibrium Crooks temperature, which enters in the asymmetry function, as indicated by Eq. (8).

As already discussed, if we want this technique to be applicable to the design of nonequilibrium thermodynamic

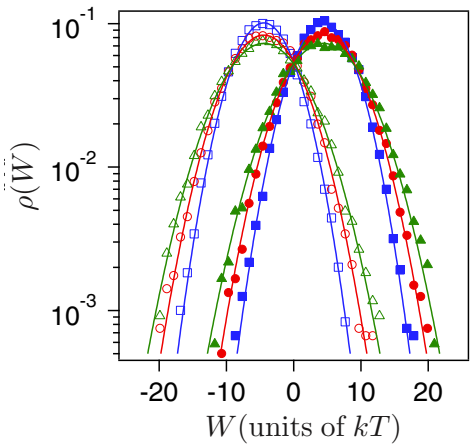

FIG. 4. (Color online) Work distributions in the forward [$\rho(W)$, filled symbols] and backward [$\tilde{\rho}(-W)$, open symbols] dragging experiments depicted in Fig. 2. Different symbols and colors correspond to different noise intensities, yielding the following values of the Crooks temperature: $T_c = 525$ K (blue squares) $T_c = 775$ K (red circles), and $T_c = 1010$ K (green triangles). Solid lines are the theoretical values of the work distributions obtained for the same values of kinetic temperatures. Work was calculated from trajectories sampled at $f = 10$ kHz.

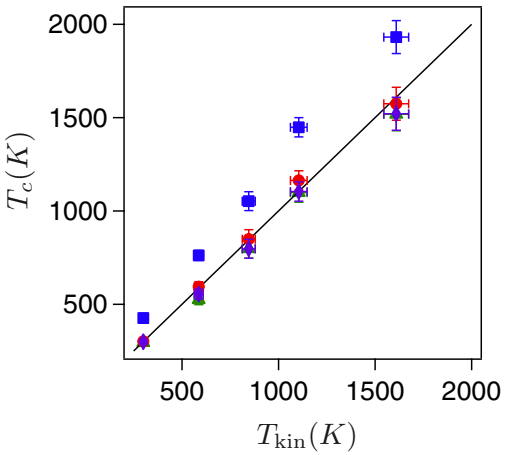

FIG. 5. (Color online) Effective nonequilibrium kinetic temperature, T_c, vs effective equilibrium kinetic temperature, $T_{\rm kin}$, for different amplitudes of the external noise. Different symbols correspond to results obtained for different sampling rates: 1 kHz (blue squares), 2 kHz (red circles), 5 kHz (green triangles), and 10 kHz (magenta diamonds). Solid black line corresponds to $T_c = T_{\rm kin}$. Error bars represent statistical errors with a statistical significance of 90%.

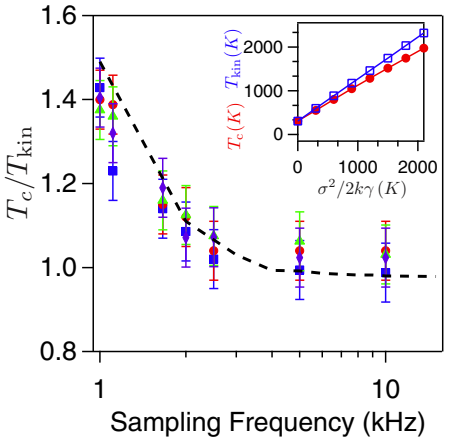

FIG. 6. (Color online) Values of the quotient $T_c/T_{\rm kin}$ in the dragging experiment as functions of the sampling frequency for different values of the external field, corresponding to the kinetic temperatures: $T_{\rm kin} = 525$ K (blue squares), $T_{\rm kin} = 775$ K (red circles), $T_{\rm kin} = 1010$ K (green triangles), and $T_{\rm kin} = 1520$ K (magenta diamonds). We also show the value of $T_c/T_{\rm kin}$ as a function of the sampling frequency obtained from numerical simulations of the overdamped Langevin equation for an external noise with flat spectrum up to $f_{\rm co} = 3$ kHz and intensity $\sigma^2/2k\gamma = 500$ K (black dashed curve). Inset: $T_{\rm kin}$ (open blue squares) and T_c (red filled circles) as a function of noise intensity, $\sigma^2/2k\gamma$, for the experimental values of the experiment described in Ref. [11], where $f_{\rm co} = 1$ kHz and the acquisition frequency $f = 20$ kHz. Solid lines are included to guide the eye.

processes, one would require that the equilibrium and nonequilibrium kinetic temperatures, that is, $T_{\rm kin}$ and T_c, to coincide within experimental errors. However, some discrepancies were found in Ref. [11] when the sampling frequency was changed, and their origin could not be fully understood.

In order to clarify this issue, we now compare the values of $T_{\rm kin}$ and T_c obtained for different values of the noise amplitude and different acquisition frequencies, ranging from 1 to 10 kHz. Figure 5 shows that equilibrium and nonequilibrium effective temperatures do coincide within experimental errors when the sampling rate exceeds $f = 2$ kHz. $T_{\rm kin}$ is measured from the variance of the position of the particle [Eq. (2)] from a time series of 20 s in which the trap is held fixed, yielding the very same value in the analyzed range of sampling frequency. When changing the position acquisition frequency, the value of $T_{\rm kin}$ does not change, whereas T_c changes significantly up to a saturating value, reached when $f \simeq 2$ kHz.

We can get a deeper understanding of the mismatch between $T_{\rm kin}$ and T_c by simulating the overdamped Langevin equation (1) and taking into account the characteristic frequencies of the system under study. We can identify three such frequencies, namely, the corner frequency of the trap, a low-frequency electrophoretic relaxation, and the cutoff of the amplifier. The first one is given by the quotient between the stiffness of the trap and the viscosity of the medium, $f_c = \frac{\kappa}{2\pi\gamma} = 340$ Hz in this case, and is related to the characteristic time $\tau_r = \gamma/\kappa$ below which the motion of the particle is purely diffusive. The referred electrophoretic process is the α or concentration polarization mechanism, defining a frequency f_α above which the electrophoretic response decreases due to a relaxation of the polarization state of the particle and its electric double layer. This relaxation is typically in the kHz range for micron-sized particles [41,42]. Finally, the electric field is applied in the chamber though an amplifier with a finite bandwidth of 10 kHz. Since the last two are very close, they cannot be resolved, but a cutoff of the random force at $f_{\rm co} = 3$ kHz was recently observed in Ref. [33] with the same experimental setup used here.

We performed numerical simulations of the overdamped Langevin equation (1) using an Euler numerical simulation scheme, with a simulation time step of $\delta t = 10^{-3}$ ms. The values of all the physical parameters are set to those of the experiment. The spectrum of the external force is flat up to a cutoff frequency of $f_{\rm co} = 3$ kHz, and its amplitude is arbitrarily set to a value σ such that $\sigma^2/2k\gamma = 500$ K. The random force was obtained generating a Gaussian white noise signal and applying a filter with a cutoff frequency $f_{\rm co} = 3$ kHz, followed by an inverse Fourier transform.

Figure 6 shows the values of the quotient $T_c/T_{\rm kin}$ as a function of the sampling frequency plotted for different values of the external field (different symbols in the Figure) corresponding to those indicated in the caption of Fig. 5. The dashed black line in Fig. 6 shows that the value of $T_c/T_{\rm kin}$ as a function of the sampling frequency, as obtained from the numerical simulations, is in good agreement with the experimental measurements.

When sampling close to the corner frequency of the trap, f_c, equilibrium and nonequilibrium kinetic temperatures do not coincide, and T_c is above its equilibrium counterpart, $T_c > T_{\rm kin}$. This result can be understood from the fact that the Brownian fluctuations of the position of the particle cannot be sampled accurately when $f \gtrsim f_c$. The poor statistics of the position results in wrong estimates of the work fluctuations in our nonequilibrium experiments. The work distributions are Gaussian for all the sampling frequencies considered in this

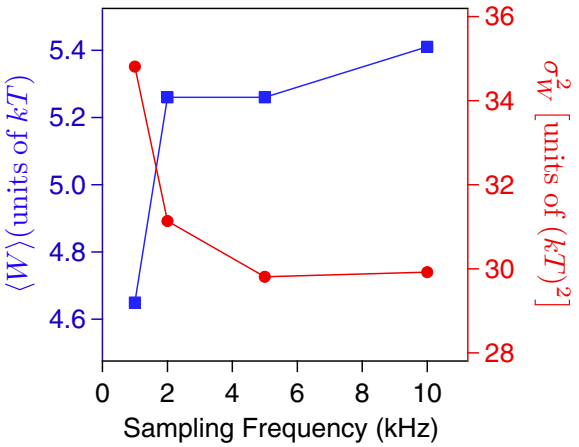

FIG. 7. (Color online) Average of the work distributions (blue squares, left axis) and variance (red circles, right axis) for the dragging process at positive velocity described by the protocol shown in Fig. 2 as a function of the sampling frequency. Solid lines are a guide to the eye.

work and therefore can be fully characterized by their mean and variance. For Gaussian work distributions, T_c is proportional to the quotient between the variance σ_W^2 and the mean $\langle W\rangle$ of the distribution of the forward process [11]

$$T_c = \frac{\sigma_W^2}{2k\langle W\rangle}. \tag{11}$$

Figure 7 shows the values of the mean and the variance of the work in the dragging (forward) experiment as functions of the sampling frequency. The average work increases with the sampling frequency, as predicted in Ref. [43]. On the other hand, the variance of the work decreases when increasing the data higher acquisition rate. As a result, the quotient between the variance and the mean, and hence T_c, decreases with the sampling frequency, as shown in Fig. 6.

For sampling rates above the cutoff frequency, $f \geqslant f_{\rm co} = 3$ kHz, we observe that T_c lies below $T_{\rm kin}$, as shown in Fig. 6. This underestimation of T_c appears because of the missing forcing at frequencies above the cutoff. Interestingly, stronger deviations on this side ($T_c < T_{\rm kin}$) were reported in Ref. [11] for a similar dragging trap experiment, where the sampling frequency, $f = 20$ kHz, was well above the cutoff frequency of the noise, $f_{\rm co} = 1$ kHz in that case. From the experimental point of view, we may note that in the present work the noise cutoff frequency given by the amplifier is one order of magnitude larger than the one in Ref. [11], and therefore the drawbacks of a colored spectrum of the noise are reduced [33]. In the inset in Fig. 6, we show the results of simulations of Langevin equation for the experimental conditions used in Ref. [11] ($f_{\rm co} = 1$ kHz, $\kappa = 6\,{\rm pN}/\mu{\rm m}$, $\tau_1 = \tau_2 = 6.3$ ms, and $L = 122$ nm, for instance), which confirm the experimental result $T_c < T_{\rm kin}$ for high sampling rates.

From this discussion, we can conclude that a sampling frequency $f = 2$ kHz is optimal for the experiment we describe next, since it is significantly above the corner frequency ($f_c \sim 300$ Hz) to ensure that we observe Brownian fluctuations and below any relaxation of the external force ($f_{\rm co} \sim 3$ kHz),

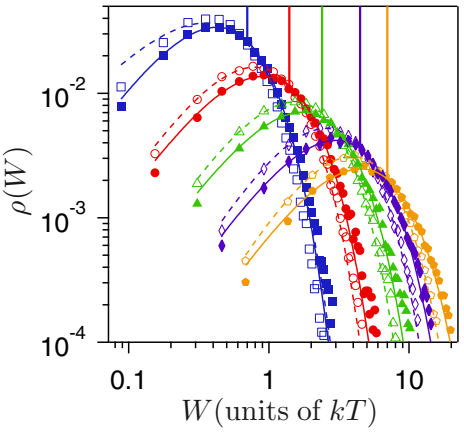

FIG. 8. (Color online) Work distributions in the isothermal compression [$\rho(W)$, filled symbols] and isothermal expansion [$\tilde{\rho}(-W)$, open symbols] for different values of the noise intensities corresponding to the following nonequilibrium effective temperatures: Without external field, $T_c = 300$ K (blue squares), $T_c = 610$ K (red circles), $T_c = 885$ K (green triangles), $T_c = 1920$ K (magenta diamonds), and $T_c = 2950$ K (orange pentagons). Solid and dashed curves are fits to Eqs. (12) and (13), respectively. Vertical lines of the corresponding colors show the expected value for the free energy change at the given temperatures. Data acquisition rate to calculate the work: $f = 2$ kHz.

which yields a correct characterization of nonequilibrium work fluctuations.

B. Isothermal compression and expansion

The distributions of the work (minus the work) in the forward (backward) process of increasing (decreasing) the stiffness of the trap (see Fig. 3) obtained using the optimal frequency $f = 2$ kHz and for different values of the external noise amplitude are shown in Fig. 8. We notice that the work fluctuations are non-Gaussian for both isothermal compression and expansion, as predicted theoretically [44]. The distributions can be fitted with a very good agreement to generalized Gamma distributions,

$$\rho(W) = C_F\, W^{z_F}\, e^{-W/\alpha_F}, \tag{12}$$

$$\tilde{\rho}(-W) = C_B\, (-W)^{z_B}\, e^{W/\alpha_B}, \tag{13}$$

where the fitting parameters C_F, C_B, α_F, and α_B depend on the amplitude of the external noise, but not z_F and z_B (data not shown). The above result can be justified provided that the work along isothermal compression and expansion is equal to the sum of squared Gaussian variables [see Eq. (10)] which is Gamma distributed [45,46]. Interestingly, the distributions (12) and (13) are analogous to that of the work in the adiabatic compression or expansion of a dilute gas [47].

The asymmetry between forward (compression) and backward (expansion) work distributions is an indicator of the irreversibility or the nonequilibrium nature of the process [25]. In Fig. 8 we show that the forward and backward work histograms cross at the value of the effective free energy change $\Delta F = kT_{\rm kin} \ln\sqrt{\kappa_{\rm fin}/\kappa_{\rm ini}}$ in all cases, with $T_{\rm kin}$ equal to the equilibrium kinetic temperature, measured in an independent equilibrium experiment. We measure the difference between

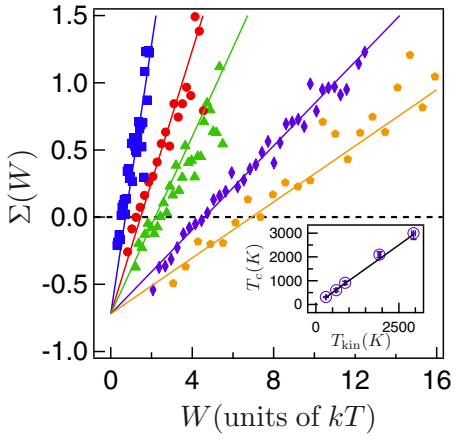

FIG. 9. (Color online) Experimental values (markers) and theoretical values (solid lines) of the work asymmetry function obtained from the work distributions in Fig. 8. Theoretical curves are computed using the values obtained for $T_{\rm kin}$. Inset: T_c as a function of $T_{\rm kin}$ (open magenta circles, error bars are smaller than the symbol size). The solid line has slope 1.

$\rho(W)$ and $\tilde{\rho}(-W)$ with the work asymmetry function [Eq. (6)], whose values for different noise intensities are shown in Fig. 9. The work asymmetry function depends linearly on the work, with its slope equal to $1/kT_{\rm kin}$, or equivalently $T_c = T_{\rm kin}$. The inset in Fig. 9 shows that this equality holds throughout the range of temperatures we explored. This result implies that our setup, when sampling at $f = 2$ kHz, is suitable to implement nonequilibrium isothermal compression or expansions in the mesoscale, with the externally controlled temperature verifying all the requirements of an actual one.

V. CONCLUSIONS

In this paper we have studied the dynamics of an optically trapped microsphere immersed in water and subject to an external colored noise with flat spectrum up to a finite cutoff frequency. We have shown that, under these conditions, the fluctuations of the work in a nonequilibrium process define a temperature that coincides with the kinetic temperature of a particle in a thermal bath as obtained from equilibrium measurements. This fact has been tested experimentally in two different nonequilibrium processes. First, dragging the trap at constant speed and, second, changing the trap stiffness linearly with time. In the second case we have found that the work fluctuations are non-Gaussian and fit well to a generalized Gamma function.

The agreement between the temperature obtained from work fluctuations under a nonequilibrium driving and the kinetic temperature obtained in equilibrium is only found when the work is calculated using a sampling rate significantly greater than the corner frequency of the trap and below the cutoff frequency of the noise, $f = 2$ kHz being an optimal choice for the experimental conditions of the present work.

The main application of the experimental setup we introduced will be the construction of thermodynamic heat engines at the mesoscale where the temperature of the system can be arbitrarily switched. Interestingly, we have been able to extend by orders of magnitude the temperature range at which these motors can perform [4,5]. This opens the possibility for the design of nonequilibrium processes following the theoretical proposals in Refs. [48–54].

ACKNOWLEDGMENTS

We acknowledge fruitful discussions with J. M. R. Parrondo, Luis Dinis, and Dmitry Petrov. All authors acknowledge financial support from the Fundació Privada Cellex Barcelona, Generalitat de Catalunya Grant No. 2009-SGR-159, and from the MICINN (Grant No. FIS2011-24409). E.R. acknowledges financial support from the Spanish Government (ENFASIS) and Max Planck Institute for the Physics of Complex Systems. A.O. acknowledges support from the Consejo Nacional de Ciencia y Tecnología and from Tecnológico de Monterrey (Grant No. CAT-141).

[1] U. Seifert, Rep. Prog. Phys. **75**, 126001 (2012).
[2] G. Volpe, S. Perrone, J. M. Rubi, and D. Petrov, Phys. Rev. E **77**, 051107 (2008).
[3] G. M. Wang, E. M. Sevick, E. Mittag, D. J. Searles, and D. J. Evans, Phys. Rev. Lett. **89**, 050601 (2002).
[4] E. Roldán, I. A. Martínez, J. M. R. Parrondo, and D. Petrov, Nature Phys. **10**, 457 (2014).
[5] V. Blickle and C. Bechinger, Nature Phys. **8**, 143 (2012).
[6] R. Yasuda, H. Noji, K. Kinosita Jr., and M. Yoshida, Cell **93**, 1117 (1998).
[7] H. Mao, J. Ricardo Arias-Gonzalez, S. B. Smith, I. Tinoco Jr., and C. Bustamante, Biophys. J. **89**, 1308 (2005).
[8] J. Millen, T. Deesuwan, P. Barker, and J. Anders, Nature Nanotech. **9**, 425 (2014).
[9] K. Sekimoto, *Lecture Notes in Physics* (Springer, Berlin, 2010), Vol. 799.
[10] J. R. Gomez-Solano, L. Bellon, A. Petrosyan, and S. Ciliberto, Europhys. Lett. **89**, 60003 (2010).
[11] I. A. Martínez, É. Roldán, J. M. R. Parrondo, and D. Petrov, Phys. Rev. E **87**, 032159 (2013).
[12] G. E. Crooks, Phys. Rev. E **60**, 2721 (1999).
[13] I. Santamaria-Holek and A. Pérez-Madrid, J. Phys. Chem. B **115**, 9439 (2011).
[14] B. Abou and F. Gallet, Phys. Rev. Lett. **93**, 160603 (2004).
[15] N. Greinert, T. Wood, and P. Bartlett, Phys. Rev. Lett. **97**, 265702 (2006).
[16] J. R. Gomez-Solano, A. Petrosyan, and S. Ciliberto, Phys. Rev. Lett. **106**, 200602 (2011).
[17] C. Song, P. Wang, and H. A. Makse, Proc. Natl. Acad. Sci. USA **102**, 2299 (2005).
[18] D. Loi, S. Mossa, and L. F. Cugliandolo, Phys. Rev. E **77**, 051111 (2008).
[19] P. Martin, A. Hudspeth, and F. Jülicher, Proc. Natl. Acad. Sci. USA **98**, 14380 (2001).
[20] A. Ashkin, Phys. Rev. Lett. **24**, 156 (1970).

[21] F. Evers, C. Zunke, R. D. L. Hanes, J. Bewerunge, I. Ladadwa, A. Heuer, and S. U. Egelhaaf, Phys. Rev. E **88**, 022125 (2013).
[22] M. S. Simon, J. M. Sancho, and K. Lindenberg, Phys. Rev. E **88**, 062105 (2013).
[23] J. Gieseler, R. Quidant, C. Dellago, and L. Novotny, Nature Nanotech. **9**, 358 (2014).
[24] G. Volpe, L. Kurz, A. Callegari, G. Volpe, and S. Gigan, Opt. Express **22**, 18159 (2014).
[25] E. Roldán, *Irreversibility and Dissipation in Microscopic Systems* (Springer, Berlin, 2014).
[26] S. Raj, M. Marro, M. Wojdyla, and D. Petrov, Biomed. Opt. Expr. **3**, 753 (2012).
[27] S. Rao, S. Raj, B. Cossins, M. Marro, V. Guallar, and D. Petrov, Biophys. J. **104**, 156 (2013).
[28] P. Gross, N. Laurens, L. B. Oddershede, U. Bockelmann, E. J. Peterman, and G. J. Wuite, Nature Phys. **7**, 731 (2011).
[29] Q. Lu, A. Terray, G. E. Collins, and S. J. Hart, Lab Chip **12**, 1128 (2012).
[30] I. Semenov, S. Raafatnia, M. Sega, V. Lobaskin, C. Holm, and F. Kremer, Phys. Rev. E **87**, 022302 (2013).
[31] F. Strubbe, F. Beunis, T. Brans, M. Karvar, W. Woestenborghs, and K. Neyts, Phys. Rev. X **3**, 021001 (2013).
[32] A. Jons and P. Zemnek, Electrophoresis **29**, 4813 (2008).
[33] É. Roldán, I. A. Martínez, L. Dinis, and R. A. Rica, Appl. Phys. Lett. **104**, 234103 (2014).
[34] I. A. Martínez, É. Roldán, L. Dinis, D. Petrov, and R. A. Rica (unpublished).
[35] P. Langevin, C. R. Acad. Sci. Paris **146** (1908).
[36] D. Collin, F. Ritort, C. Jarzynski, S. Smith, I. Tinoco, and C. Bustamante, Nature (London) **437**, 231 (2005).
[37] N. Garnier and S. Ciliberto, Phys. Rev. E **71**, 060101 (2005).
[38] M. Tonin, S. Bálint, P. Mestres, I. A. Martìnez, and D. Petrov, Appl. Phys. Lett. **97**, 203704 (2010).
[39] K. Berg-Sørensen and H. Flyvbjerg, Rev. Sci. Instrum. **75**, 594 (2004).
[40] A. Saha, S. Lahiri, and A. M. Jayannavar, Phys. Rev. E **80**, 011117 (2009).
[41] C. Grosse and A. Delgado, Curr. Opin. Colloid Interface Sci. **15**, 145 (2010).
[42] R. A. Rica, M. L. Jiménez, and Á. V. Delgado, Soft Matter **8**, 3596 (2012).
[43] A. Gomez-Marin, J. M. R. Parrondo, and C. Van den Broeck, Phys. Rev. E **78**, 011107 (2008).
[44] T. Speck, J. Phys. A **44**, 305001 (2011).
[45] J. Sung, Phys. Rev. E **76**, 012101 (2007).
[46] N. G. Van Kampen, *Stochastic Processes in Physics and Chemistry* (Elsevier, North-Holland, Amsterdam, 1992), Vol. 1.
[47] G. E. Crooks and C. Jarzynski, Phys. Rev. E **75**, 021116 (2007).
[48] T. Hondou and K. Sekimoto, Phys. Rev. E **62**, 6021 (2000).
[49] M. Esposito, R. Kawai, K. Lindenberg, and C. Van den Broeck, Phys. Rev. Lett. **105**, 150603 (2010).
[50] T. Schmiedl and U. Seifert, Europhys. Lett. **81**, 20003 (2008).
[51] S. Rana, P. Pal, A. Saha, and A. M. Jayannavar, arXiv:1404.7831.
[52] P. S. Pal, S. Rana, A. Saha, and A. M. Jayannavar, Phys. Rev. E **90**, 022143 (2014).
[53] G. Verley, T. Willaert, C. Van de Broeck, and M. Esposito, arXiv:1404.3095.
[54] A. Dechant, N. Kiesel, and E. Lutz, arXiv:1408.4617.